Theory of Strain Birefringence Based on a Realistic Model of Rubberlike Elasticity

Vasilios Galiatsatos

Research Division, The Goodyear Tire & Rubber Company, Akron, Ohio 44305

Received December 15, 1989

ABSTRACT: A new theory of strain birefringence of amorphous networks is presented. The theory is based on the constrained chain model of rubberlike elasticity recently developed by Erman and Monnerie. The quantitative treatment is molecular in nature and uses two adjustable parameters in order to fully describe the dependence of birefringence on deformation. The constrained chain theory and the birefringence of phantom networks are briefly reviewed with emphasis on the points relevant to strain birefringence. The contribution of the topological constraints to birefringence is developed, as well as the dependence of birefringence on stress. Illustrative calculations document the results for an unswollen tetrafunctional network prepared in bulk. Final comments include remarks on the connection of the adjustable parameters of the theory to molecular characteristics.

Introduction

The molecular origins of rubberlike elasticity suggest that the thoroughly studied models of phantom and affine networks constitute only an approximation to real networks.[1] Consequently, the various models developed to quantitatively describe the behavior of amorphous networks have concentrated on the role of interchain interactions on the elastic free energy of the network.[1,2]

Carefully designed experimental methods are therefore needed to provide the framework for a systematic evaluation of all the theories of rubberlike elasticity put forth. Strain-birefringence methods have been used to properly characterize the stress–optical behavior of cross-linked model and random polymers,[3–5] to test the various postulates of rubberlike elasticity,[6] and, finally, to confirm the predictions of the rotational isomeric state theory.[7]

The premises of the strain-birefringence theory are based on the pioneering work of Kuhn and Grün,[8] Volkenstein,[9] Treloar,[10] and Flory.[11] Until recently, simple molecular models have been used to develop the theory for amorphous polymer networks. The advancement of the new rubberlike elasticity models has, however, necessitated the introduction of the new concepts to the theories governing strain birefringence. The development of the constrained junction theory has therefore led to a model of strain birefringence that takes into account the effect of the topological constraints present in the network.[6]

The newly developed modification of the constrained junction theory, termed the constrained chain theory,[14] is a major departure from the older theory since it introduces the effects of the constraints not only on the junctions but also along the contour of the network chain. This paper presents a theory of strain birefringence based on the concepts introduced in the constrained chain theory. It represents an effort to understand the relationship of birefringence to stress for deformed networks as well as an effort to quantitatively predict the values of the stress–optical coefficient.

The first section reviews the relevant points of the constrained junction and constrained chain theories and describes the use of the adjustable parameters introduced in these models. Next, the birefringence behavior of phantom networks is outlined, since this type of network forms the basis for the description of the behavior of real networks. The influence of topological constraints on birefringence is examined in the third section, where equations for the contribution of the constraints and their domains are developed. The combination of phantom network theory with constraint theory is described in the section establishing the birefringence of real networks. Finally, the development of equations that describe the relationship of birefringence to stress is presented. Numerical calculations depict representative results for a tetrafunctional network prepared in the bulk. Concluding remarks focus on the role of the parameters introduced in the model and the ramifications of their use.

Review of the Rubberlike Elasticity Theory for Real Networks

In this section we give a concise description of the relevant points of the constrained junction and the constrained chain theories. The two theories represent departures from the simpler models of the phantom and the affine networks, by realistically incorporating the effect of topological constraints in the calculation of the elastic free energy of the network. We focus on the concepts relevant to the development of the strain-birefringence theory discussed in the following sections. A number of excellent references are available for a more detailed introduction to the subject (refs 1 and 2 and references therein).

The constrained junction theory first developed by Flory[12] and subsequently by Erman and Flory[13] has emerged as a most successful effort to describe the molecular origins of rubberlike elasticity. The theory considers the action of the topological constraints and its effect on the derived mechanical properties of the network. The model demonstrates quantitative agreement with data from uniaxial elongation[13] and swelling experiments.[13] The two adjustable parameters governing the behavior of the model are κ and ζ. κ is defined as[12,13]

$$\kappa = \frac{\langle(\Delta R)^2\rangle_0}{\langle(\Delta s)^2\rangle_0} \tag{1}$$

where $\langle(\Delta R)^2\rangle_0$ represents the mean-squared fluctuations of junctions in the phantom network (reference state). $\langle(\Delta s)^2\rangle_0$ denotes the mean-squared fluctuations of junctions from their mean positions in the reference state under the action of constraints only.

For a phantom network $\kappa = 0$, since there are no restrictions in the fluctuations and therefore to the values

0024-9297/90/2223-3817$02.50/0

of the quantity $\langle(\Delta s)^2\rangle_0$. In the case of the affine network on the other hand, the constraints are infinitely strong, $\langle(\Delta s)^2\rangle_0 = 0$ and κ reaches infinity.

Introduction of the second parameter, ζ, allows quantitative predictions of experimental data. The presence of this parameter was directed by the fact that the moduli of the network samples decrease much faster than that predicted when only one parameter (κ) is used.[13] This decrease is observed when the samples are elongated or swelled by a diluent. The connection of parameter ζ to molecular characteristics is not established.

As the name of the theory implies, the multifunctional cross-linking sites (junctions) are the only parts of the network chains where the constraints have an explicit effect. Restrictions of the fluctuations along the chains are assumed to be contained in the junction constraints. It has been noted though that chain–chain interactions may be important.[12]

Recently, Erman and Monnerie presented an elegant extension to the constrained junction theory.[14] The new treatment, referred to as the constrained chain model, takes into account the restriction of chain movements along the chain contour. The theory focuses on the instantaneous distribution of the centers of mass of the chains instead of those of the junctions.

Briefly, the theory is based on the assertion, first made by Flory,[12] that only entanglements that are affected by deformation contribute to the modulus of the network. Increasing elongation is assumed to diminish the entanglements and so does swelling. The incorporation of strain-dependent entanglements modifies the instantaneous distribution of the centers of mass of the chains when these are compared to their corresponding locations in the phantom network. In their treatment, Erman and Monnerie divide the network chain into a number of (Gaussian) subchains and consider the action of the topological constraints on the end points of these subchains.

The elastic free energy due to the constraints is calculated as being equal to[14]

$$\Delta A_c = \frac{\nu kT}{2}\sum_t [B_t + D_t - \ln(1 + B_t) - \ln(1 + D_t)] \quad (2)$$

where ν is the number of network chains, k is the Boltzmann constant, and T is the temperature in degrees Kelvin.

The quantities B_t and D_t are given by

$$B_t = \frac{h(\lambda_t)^2(\lambda_t^2 - 1)}{[\lambda_t^2 + h(\lambda_t)]^2} \quad (3)$$

$$D_t = \frac{\lambda_t^2 B_t}{h(\lambda_t)} \quad (4)$$

where λ_ts are the components of the macroscopic deformation tensor and the function $h(\lambda_t)$ is given by

$$h(\lambda_t) = \frac{\kappa_G}{1 + (\lambda_t^2 - 1)\Phi} \quad (5)$$

The parameter κ_G is the only adjustable parameter of the constrained chain model, provided the cycle rank, ξ, of the network is already known. The quantity Φ is given by two alternative formulations:

$$\Phi = [1 - (2/\varphi)]^2/3 \quad (6)$$

$$\Phi = [1 - (2/\varphi)]^2 \quad (7)$$

Equation 6 holds for sufficiently long network chains only. φ is the junction functionality ($\varphi \geq 3$). The two expressions describe two different approaches to the treatment of the fluctuations of the end points of the subchains. Equation 6 developed by Kloczkowski, Erman, and Mark[15,16] is obtained when the fluctuations of the end points of the subchains are dependent on macroscopic deformation; the fluctuations of the junctions, however, are invariant to strain. Equation 7 developed independently by Pearson[17] and Ullman[18,19] is obtained when the fluctuations of the end points of the subchains are independent of macroscopic deformation.

According to the theory the elastic free energy of the network is obtained by[14]

$$\Delta A_{el} = \frac{1}{2}\xi kT\sum_t\left[(\lambda_t^2 - 1) + \left(\frac{\nu}{\xi}\right)[B_t - D_t - \ln(1 + B_t) - \ln(1 + D_t)]\right] \quad (8)$$

It should be noted that eq 8 reduces to the elastic free energy of the phantom network when κ_G is equal to zero. On the other hand, when κ_G approaches infinitely large values, the elastic free energy reduces to a value that is greater than that of the affine network. This is in contrast with results obtained by the constrained junction theory, where the affine network is the upper limit for the elastic free energy values.[12,13]

Birefringence of Phantom Networks

In this section we describe the theory of birefringence for phantom networks. The presented treatment follows closely the conventions and notation of refs 1 and 6 for reasons of brevity and consistency.

Consider the instantaneous end-to-end distance r for the ith network chain at equilibrium and at fixed strain. For a perfect phantom network the birefringence induced because of a deformation is defined as[1]

$$\Delta n = \left(\frac{2\pi}{27}\right)\left(\frac{\nu}{V}\right)\left[\frac{(n^2 + 2)^2}{n}\Gamma_2\right]\left[\Lambda_x^2 - \frac{(\Lambda_y^2 + \Lambda_z^2)}{2}\right] \quad (9)$$

Λ_ts are the components of the molecular deformation tensor, which is given by[1]

$$\Lambda_t^2 = [1 - (2/\varphi)]\lambda_t^2 + (2/\varphi) \qquad t = x, y, z \quad (10)$$

where λ_ts are the components of the macroscopic deformation tensor.

The quantity Γ_2 is defined as

$$\Gamma_2 = \frac{9}{10}\sum_i \frac{\langle \mathbf{r}^T \hat{\alpha}_i \mathbf{r}\rangle_0}{\langle r^2\rangle_0} \quad (11)$$

The summation is over all the units forming the chain. $\hat{\alpha}_i$ is the anisotropic part of the polarizability tensor for the unit with index i. $\mathbf{r}^T$ is the transpose vector of the end-to-end vector $\mathbf{r}$, and the subscript "0" signifies that the average is over all configurations of the free chain. It is assumed that the polarizability tensor for the chain with a given configuration is obtained as the sum of the polarizability tensors of the groups forming the chain.[9,11]

The connection between the polarizability tensor and the parameter Γ_2 is given by[9]

$$\left[\alpha_{xx} - \frac{(\alpha_{yy} + \alpha_{zz})}{2}\right]_r = \Gamma_2\frac{x^2 - [(y^2 + z^2)/2]}{\langle r^2\rangle_0} \quad (12)$$

and $\langle r^2\rangle_0$ is the mean-squared end-to-end distance of a free chain. α_{xx}, α_{yy}, and α_{zz} are the x, y, and z components of the tensor α_i for the chain averaged over all

configurations. The subscript r on the left side of eq 12 signifies that the averaging is for the chain with fixed ends.

Combining eqs 9 and 10, we obtain for the birefringence of a phantom network

$$\Delta n_{ph} = \left(\frac{\xi}{V}\right) kTC\left[\lambda_x^2 - \frac{(\lambda_y^2 + \lambda_z^2)}{2}\right] \quad (13)$$

Focusing on the birefringence along the two principal axes, x and y, we obtain

$$\Delta n_{xy} = \left(\frac{2\pi\nu}{27V}\right)\left(1 - \frac{2}{\varphi}\right)\left[\frac{(n^2+2)^2\Gamma_2}{n}\right](\lambda_x^2 - \lambda_y^2) \quad (14)$$

For the development of eq 13 we have used the expression for the quantity C, the stress-optical coefficient, which is given by[6,11]

$$C = \frac{2\pi}{27kT}\frac{(n^2+2)^2}{n}\Gamma_2 \quad (15)$$

and n is the mean refractive index of the network. The stress-optical coefficient is the proportionality constant between the birefringence Δn_{xy} and the difference between the true stresses along the same axes:

$$C = \Delta n_{xy}/(\tau_x - \tau_y) \quad (16)$$

Contribution of Topological Constraints to the Birefringence

The contribution of the topological constraints on the molecular deformation tensor is[6]

$$\Lambda_t^2 = (2/\varphi)B_t \qquad t = x, y, z \quad (17)$$

The contribution due to the constraints to the birefringence as a result of the molecular deformation is then given by[6]

$$\Delta n'_{xy,c} = (\nu/V)kTC(\Lambda_{x,c}^2 - \Lambda_{y,c}^2) \quad (18)$$

Substituting eq 17 in eq 18, we obtain

$$\Delta n'_{xy,c} = (2/\varphi)(\nu/V)kTC(B_x - B_y) \quad (19)$$

Equation 19 expresses the effect of the deformation of network chain vectors on birefringence.

There is, however, one more type of contribution necessary to consider.[6] As a result of the alteration of the dimensions of the network chains because of the applied strain, one should also expect the ends of the Gaussian subchains to move correspondingly. Assuming that these ends and their corresponding domains behave like elastically coupled elements, movements of the ends should induce a response from the domains. This mutual interaction contributes to the free energy of the system and therefore to the stress.

The fact that the system chain end/domain reacts to the applied macroscopic strain makes reasonable the assertion that the resulting orientation contributes to the birefringence. This orientation is in addition to the orientation resulting from the relocation and distortion of the domains due to the distortion of the environment surrounding them and whose contribution is incorporated in eqs 18 and 19.

We characterize the reaction of the domain to the action of the subchain end as being given by the ratio[6]

$$\frac{\langle(\Delta s_{*t})^2\rangle_{\lambda_t}}{\langle(\Delta s_t)^2\rangle_{\lambda_t}} \quad (20)$$

where the average is over all subchain ends. $\langle(\Delta s_t)^2\rangle$ represents the components, along the principal axes of the strain, of the tensor of second moments of the fluctuations of the "free" subchain ends. The characterization of the constraints within the domains by this tensor was first put forth by Flory and Erman.[6] The subscript "λ_t" denotes that the domain deforms due to the applied strain. The quantity $\langle(\Delta s_{*t})^2\rangle$ characterizes the actual moments of the subchain ends displacement.

The ratio given in expression 20 has been previously identified[12] with the inverse ratio of two parameters from the constrained junction theory. The parameters are (a) the Gaussian distribution of the components Δs_t for hypothetical "free" junctions, denoted by σ_λ, and (b) the distribution for junctions in the real network, denoted by $\sigma_{*\lambda}$. Corresponding parameters appear in the constrained chain theory.[14] Subsequently we have that

$$\frac{\langle(\Delta s_{*t})^2\rangle_{\lambda_t}}{\langle(\Delta s_t)^2\rangle_{\lambda_t}} = \frac{\sigma_\lambda}{\sigma_{*\lambda}} \quad (21)$$

According to the theory the ratio $\sigma_\lambda/\sigma_{*\lambda}$ is given by[14]

$$\sigma_\lambda/\sigma_{*\lambda} = 1 + D_t \quad (22)$$

Given that parameter D_t is related to parameter B_t through eq 4, we obtain through substitution into eq 22

$$\sigma_\lambda/\sigma_{*\lambda} = 1 + \lambda_t^2 B_t[h(\lambda_t)]^{-1} \quad (23)$$

Substitution of eq 23 into eq 20 yields

$$\frac{\langle(\Delta s_{*t})^2\rangle_{\lambda_t}}{\langle(\Delta s_t)^2\rangle_{\lambda_t}} = 1 + \lambda_t^2 B_t[h(\lambda_t)]^{-1} \quad (24)$$

Comparison of eq 24 with the corresponding relation for the constrained junction theory reveals that the function g_t has now been replaced by the term $\lambda_t^2[h(\lambda_t)]^{-1}$. The function g_t is given as[12,13]

$$g_t = \lambda_t^2[\kappa^{-1} + \zeta(\lambda_t - 1)] \quad (25)$$

Assuming that the orientation of chains due to the relocation of the subchain ends within their domains of constraint is similar to the orientation of the chain vectors described earlier, we have

$$\Delta n''_{xy,c} = b(\nu/V)kTC(\lambda_x^2 B_x[h(\lambda_x)]^{-1} - \lambda_y^2 B_y[h(\lambda_y)]^{-1}) \quad (26)$$

where ν is the number of chains.

Parameter b requires special attention. Its introduction has no direct molecular connection. It is used, however, as a recognition of the difficulty to accurately describe the reactions of the constraints and the subsequent contribution to the birefringence. The values of b should lie within the range [0,1].[6]

The linear combination of eqs 19 and 26 yields the total contribution to the birefringence arising from the topological constraints. We specifically have

$$\Delta n_{xy,c} = (2/\varphi)(\nu/V)kTC(B_x - B_y) + b[\nu/V]kTC(\lambda_x^2 B_x[h(\lambda_x)]^{-1} - \lambda_y^2 B_y[h(\lambda_y)]^{-1}) \quad (27)$$

Simple algebraic manipulations yield

$$\Delta n_{xy,c} = \left(\frac{\xi}{V}\right)kTC\left(\frac{1}{1 - [2/\varphi]}\right)\left[\left(\frac{2}{\varphi}\right)(B_x - B_y) + b(\lambda_x^2 B_x h(\lambda_x)^{-1} - \lambda_y^2 B_y h(\lambda_y)^{-1})\right] \quad (28)$$

where the relation

$$\xi = \nu/[1 - (2/\varphi)] \quad (29)$$

was used in eq 28.

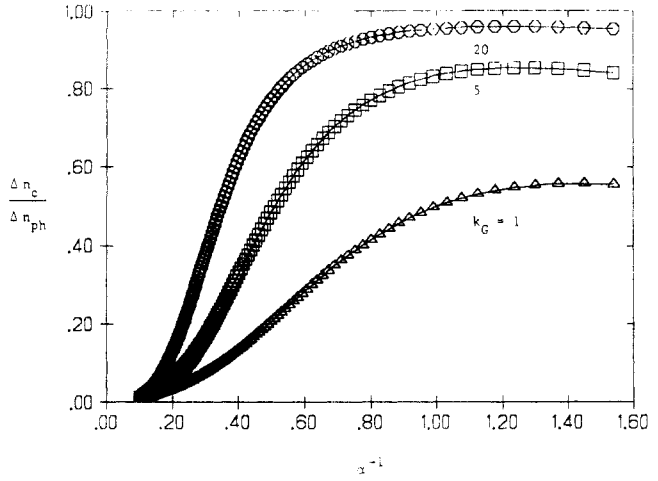

Figure 1.

Birefringence of Real Networks

The total birefringence for a real network is the linear combination of the contributions resulting from the phantom network and the contributions arising from the constraints.[6] The ratio of the birefringence due to constraints to the birefringence of the phantom network therefore is

$$\frac{\Delta n_{xy,c}}{\Delta n_{xy,ph}} = [(2/\varphi)(B_x - B_y) + b[\lambda_x^2 B_x h(\lambda_x)^{-1} - \lambda_y^2 B_y h(\lambda_y)^{-1}]]\left(\frac{1}{1-(2\varphi)}\right)\left(\frac{1}{\lambda_x^2 - \lambda_y^2}\right) \quad (30)$$

where eqs 13 and 28 have been employed. The total birefringence will then finally be given by

$$\Delta n_{xy} = \Delta n_{xy,ph}\left[1 + \frac{\Delta n_{xy,c}}{\Delta n_{xy,ph}}\right] \quad (31)$$

Dependence of Birefringence on Stress

The matrix of the stress tensor is given by[12]

$$\tau = 2\lambda[\partial \Delta A_{el}/\partial(\lambda^T\lambda)]\lambda^T/V \quad (32)$$

The eigenvalues of the matrix τ result in the principal components of the stress, and these are

$$\tau_t = 2[\partial \Delta A_{el}/\partial \lambda_t^2]\lambda_t^2/V \quad (33)$$

The derivative of the elastic free energy is equal to[14]

$$\frac{\partial \Delta A_{el}}{\partial \lambda_t^2} = \frac{1}{2}\xi kT\left\{1 + \frac{\nu}{\xi}[B\dot{B}(1 + B^{-1}) + D\dot{D}(1 + D^{-1})]_t\right\} \quad (34)$$

where the derivatives $\dot{B}$ and $\dot{D}$ are

$$\dot{B} = \frac{\partial B}{\partial \lambda^2} = B\left[(\lambda^2 - 1)^{-1} - 2[\lambda^2 + h(\lambda)^2]^{-1} - 2\frac{h(\lambda)^2 \lambda^2 \Phi}{\kappa_G(\lambda^2 + h(\lambda)^2)}\right] \quad (35)$$

and

$$\dot{D} = \frac{\partial D}{\partial \lambda^2} = B\left[\frac{1}{h(\lambda)^2} + \frac{\lambda^2 \phi}{\kappa_G}\right] + \frac{\lambda^2 B}{h(\lambda)^2} \quad (36)$$

By defining the function $K(\lambda^2)$ as[14]

$$K(\lambda^2) = \frac{B\dot{B}}{1+B} + \frac{D\dot{D}}{1+D} \quad (37)$$

the equation for the stress becomes

$$\tau_t = \frac{\xi kT}{V}\lambda_t^2\left[1 + \frac{\nu}{\xi}K(\lambda_t^2)\right] \quad (38)$$

The difference between the components of the stress along the principal axes x and y is then given by

$$\tau_x - \tau_y = \frac{\xi kT}{V}\left[(\lambda_x^2 - \lambda_y^2) + \left(\frac{\nu}{\xi}\right)[\lambda_x^2 K(\lambda_x^2) - \lambda_y^2 K(\lambda_y^2)]\right] \quad (39)$$

We now proceed to calculate the ratio of birefringence to stress. By using eqs 31 and 39, we obtain

$$\frac{\Delta n_{xy}}{\tau_x - \tau_y} = \left(\frac{2}{\varphi - 2}\right)(\lambda_x^2 - \lambda_y^2)^{-1}\left[(B_x - B_y) + b\left[\frac{\lambda_x^2 B_x}{h(\lambda_x)} - \frac{\lambda_y^2 B_y}{h(\lambda_y)}\right]\right]\left\{\frac{kT}{V}[\xi(\lambda_x^2 - \lambda_y^2) + \nu[\lambda_x^2 K(\lambda_x^2) - \lambda_y^2 K(\lambda_y^2)]]\right\} \quad (40)$$

Illustrative Calculations

This section presents an application of the developed theory to uniaxial extensions. A typical strain birefringence experiment involves uniaxial extension of a network sample in either the swollen or unswollen state. Application of eq 30 to this type of experimental setup yields

$$\frac{\Delta n_c}{\Delta n_{ph}} = \left\{\frac{2}{\varphi}(B_\parallel - B_\perp) + b\left[\left(\frac{\lambda^2 B}{h(\lambda)}\right)_\parallel - \left(\frac{\lambda^2 B}{h(\lambda)}\right)_\perp\right]\right\}\left[\left(\frac{1}{1-2\varphi}\right)\left(\frac{1}{\lambda_\parallel^2 - \lambda_\perp^2}\right)\right] \quad (41)$$

where the subscripts "$\parallel$" and "$\perp$" denote directions parallel and perpendicular to the axis of the applied strain.

Figure 1 gives representative results for an unswollen tetrafunctional network prepared in the bulk. The ratio $\Delta n_c/\Delta n_{ph}$ is plotted against reciprocal elongation for three values of the parameter κ_G: 1, 5, and 20. The contribution of constraints has been included to its maximum extent and as a result it is seen that for the highest value of κ_G the ratio $\Delta n_c/\Delta n_{ph}$ approaches unity. The curves have a sigmoidal shape, and they approach zero values as the inverse elongation values approach zero. Equation 6 has been used to specify the value of parameter Φ.

Conclusion

The strain birefringence theory presented here is based on a realistic model of rubberlike elasticity. The most important aspect of the theory is its molecular nature. This allows us to have a clear picture of the changes affecting birefringence.

Admittedly there are certain points that need further work in order to fully understand the connection of certain parameters (e.g., parameter b) to molecular characteristics. Clarification of the molecular mechanisms that affect the compliance of the domains of constraints to the movement of the subchain ends and junctions is also required. Alternative formulations to account for this mechanism may be needed. Contributions to orientation from local intermolecular correlations that are observed in birefringence experiments are not included in this model. Work along those lines will be invaluable.

It is needless to point out that no theory is valid unless experimental verification is in hand. Work to accomplish this is already in progress on suitable polymer networks. Detailed comparisons to other theories as well as a closer

inspection of the implications and assumptions of the theory developed here are also forthcoming. Finally, work to document the effect of swelling on birefringence using the model developed in this paper will be reported in an upcoming paper.

Acknowledgment. I thank Professors W. L. Mattice and B. E. Erman for their valuable comments. Many thanks are also due to Doreen d'Auteuil for meticulously typing the manuscript.

References and Notes

(1) Mark, J. E.; Erman, B. *Rubberlike Elasticity: A Molecular Primer*; Wiley-Interscience: New York, 1988.
(2) Queslel, J. P.; Mark, J. E. In *Comprehensive Polymer Science*; Allen, G., Ed.; Pergamon Press: Oxford, 1988.
(3) Galiatsatos, V.; Mark, J. E. *Macromolecules* **1987**, *20*, 2631.
(4) Galiatsatos, V.; Mark, J. E. *Polym. Bull.* **1987**, *17*, 197.
(5) Galiatsatos, V.; Mark, J. E. In *Advances in Silicon-Based Polymer Science*; Ziegler, J., Fearon, G., Eds.; American Chemical Society: Washington, DC, 1989.
(6) Erman, B.; Flory, P. J. *Macromolecules* **1983**, *16*, 1601.
(7) Lieberman, M. H.; Abe, Y.; Flory, P. J. *Macromolecules* **1972**, *5*, 550.
(8) Kuhn, W.; Grün, F. *Kolloid-Z.* **1942**, *101*, 248.
(9) Volkenstein, M. W. *Configurational Statistics of Polymeric Chains*; Timasheff, S. N., Timasheff, M. J., Eds.; Interscience: New York, 1963; Chapter 7.
(10) Treloar, L. R. G. *The Physics of Rubber Elasticity*, 3rd ed.; Clarendon Press: Oxford, 1975; Chapter 9.
(11) Flory, P. J. *Statistical Mechanics of Chain Molecules*; Interscience: New York, 1969.
(12) Flory, P. J. *J. Chem. Phys.* **1977**, *66*, 5720.
(13) Erman, B.; Flory, P. J. *Macromolecules* **1982**, *15*, 806.
(14) Erman, B.; Monnerie, L. *Macromolecules* **1989**, *22*, 3342.
(15) Erman, B.; Kloczkowski, A.; Mark, J. E. *Macromolecules* **1989**, *22*, 1432.
(16) Kloczkowski, A.; Mark, J. E.; Erman, B. *Macromolecules* **1989**, *22*, 1423.
(17) Pearson, D. S. *Macromolecules* **1977**, *10*, 696.
(18) Ullman, R. *J. Chem. Phys.* **1979**, *71*, 436.
(19) Ullman, R. *Macromolecules* **1982**, 15, 1393.

A One-Component Model for the Phase Behavior of Dispersions Containing Associative Polymers

Maria M. Santore, William B. Russel,* and Robert K. Prud'homme

Department of Chemical Engineering, Princeton University, Princeton, New Jersey 08544

Received October 10, 1989; Revised Manuscript Received February 16, 1990

ABSTRACT: The statistical mechanical theory developed herein predicts the effects of associative polymer, random walk chains with adhesive end groups, on the interaction between parallel plates at full and restricted equilibrium conditions. The Derjaguin approximation and Barker–Henderson perturbation theory then determine interparticle potentials and macroscopic thermodynamic variables, respectively, with the compositions of coexisting phases following from classical thermodynamic criteria for equilibrium in one-component systems. Weakly or nonassociative polymers induce depletion attractions that result in reversible phase transitions. Increasing the strength of the adhesion to the plates diminishes the range and strength of the attraction, so higher polymer concentrations are needed to induce flocculation. Sufficient adsorption to the plates may cause a repulsive barrier that stabilizes dispersions against depletion flocculation at full equilibrium. Strong adsorption, however, results in a bridging attraction that grows with polymer concentration until the surface is saturated and then diminishes with additional polymer. This leads to flocculation at low polymer concentrations and restabilization at a higher value that depends on the solvent quality. The interactions at restricted equilibrium mimic the long-range features of the full equilibrium potentials but contain an additional repulsive core.

Introduction

The role of polymers in dispersion stability and phase behavior has been a topic of interest for a number of years. Conventional systems contain homopolymers that induce phase separations via either of two mechanisms, depending on the polymer's affinity for the particle surface. It is well established both experimentally[1-4] and theoretically[1,5-7] that nonadsorbing polymer causes a volume restriction attraction and reversible phase transitions. With adsorbing homopolymers the precise mechanism for bridging flocculation remains unclear, with the most obvious explanations relying on kinetic rather than purely equilibrium effects.[8]

Our interests center on the phase behavior induced by the addition of hydrophobically modified water-soluble polymers to stable colloidal dispersions. These polymers consist of nonadsorbing water-soluble chains with grafted hydrocarbon arms (10–20 carbons long), comprising 1–2 wt % of the molecule. In aqueous solvents, the hydrophobes associate intra- and intermolecularly and adsorb reversibly onto the surface of hydrophobic particles.[9] Hydrophobically modified polymers comprise the state of the art for thickeners in the coatings industry, but their commercial use is limited by a poor understanding of their effects on the equilibrium properties of dispersions, due to the specificity of the hydrophobe adsorption. The work presented here applies not only to these new paint thickeners but also to specialty polymers employed in enhanced oil recovery and biomedical applications.

Traditionally, aqueous coatings included nonadsorbing high molecular weight polymers such as (hydroxyethyl)-

0024-9297/90/2223-3821$02.50/0